J Mater Sci (2012) 47:433–439
DOI 10.1007/s10853-011-5817-9

Chemical solution approach to $SrTiO_3$ synthesis using a new precursor

Y. Wang · L. Zhou · C. S. Li · Z. M. Yu · J. S. Li · L. H. Jin · Y. Shen · P. F. Wang · Y. F. Lu

Received: 16 April 2011 / Accepted: 21 July 2011 / Published online: 4 August 2011

Abstract We have synthesized $SrTiO_3$ (STO) using a newly developed precursor route by chemical solution approach. The new STO precursor solution was prepared in ambient atmosphere. Various characteristic methods, including thermal analyses, infrared spectroscopy, and transmission electron microscopic analyses techniques, were applied to study the thermal decomposition and crystallization behavior of STO precursor gel. The acquirement of single-phase STO powders at the different annealing atmospheres demonstrates that STO with perovskite structure is prone to tolerate the oxygen vacancies defect. Epitaxially grown STO film on textured Ni–W substrate by a seeded nucleation method shows a high *c*-axis orientation and a good out-of-plane texture. Scanning electron microscopy and atomic force microscopy investigations of STO film reveal the continuous, crack-free, and smooth surface morphology. The results suggest that STO film fabricated by the newly developed precursor route may be suitable to be used as buffer layer for subsequent growth of YBCO in coated conductors.

Y. Wang · L. Zhou · J. S. Li
State Key Laboratory of Solidification Processing, Northwestern Polytechnical University, Xi'an 710072, People's Republic of China

Y. Wang · L. Zhou · C. S. Li · Z. M. Yu · L. H. Jin · Y. F. Lu (✉)
Northwest Institute for Nonferrous Metal Research, Xi'an 710016, People's Republic of China
e-mail: wyspacestar@yahoo.com.cn

Y. Shen · P. F. Wang
Shaanxi Normal University, Xi'an 710062, People's Republic of China

Introduction

Coated conductors composed of metal substrate/buffer layer/superconducting layer/protective layer become a research focus in the high-temperature superconducting materials field because it provides the potential to support high current for electric utility and high magnetic field applications at 77 K [1–5]. A great deal of effort has been invested in the all-chemical solution deposited buffer layer and superconducting layer due to its several advantages over physical vapor deposition (PVD), for example, low cost and easy operation in order to realize the commercial application [3–5]. At present, the fabrication of superconducting layer with high-performance is relatively more mature in comparison with that of buffer layer by chemical solution deposition (CSD) method. Thereafter, lots of studies have concentrated mainly on the preparation of buffer layer by CSD method in coated conductors. The multi-layer architecture is generally adopted to realize two main functions of buffer layer, including transmitting the bi-axial texture from substrate to superconducting layer and preventing oxygen and metal atoms diffusion [3, 4]. With the increase of layer amount of buffer layer, however, its textured degree and surface quality would decrease, which results in the increase of cost and the decrease of final superconducting performance. Therefore, single buffer layer on Ni–W substrate deposited by CSD route is certain of ideal goal in respect of commercial viability. Among the oxide films presently studied, $SrTiO_3$ (STO) film offers a potential to be used as a single buffer layer for coated conductors because of its very small lattice mismatch with YBCO, low oxygen diffusivity as well as the good chemical compatibility with Ni–W substrate and YBCO [3, 4]. STO precursor solutions were synthesized from different precursors, including Strontium acetate,

Titanium alkoxide [3–12] and Strontium carbonate, Titanium isopropoxide [13], while Strontium di-i-propoxy, Titanium tetra-i-propoxy, and Niobium penta-i-propoxy precursors were used to prepare Nb-doped STO precursor solution to deposit STO films and doped STO films on single crystal substrates and metal tapes [14]. Although the perovskite structure STO provides a large lattice mismatch of 11.1% with Ni–W substrate, the good epitaxial growths are still possible for STO and doped STO films by adopting a seeded nucleation method. In addition, STO was synthesized from TiO_2 and Strontium chloride hexahydrate by hydrothermal method [15], and it was also prepared via a polymeric precursor method [16, 17].

In this article, we report a newly developed precursor solution route to synthesize STO by chemical solution approach. The advantage of this method is that the new precursor solution can be easily obtained in ambient atmosphere and the stability of this STO precursor solution is very great. The thermal decomposition and crystallization behavior of the STO precursor gel, the structural stability of STO as well as the texture and micro-structure of STO films on Ni-W substrates have been studied in detail. The results suggest that the single-phase STO powders are obtained at the different annealing atmospheres and the as-prepared STO film using the newly developed precursor solution route shows a *c*-axis oriented, continuous, crack-free as well as smooth morphology.

Experimental procedures

The newly developed STO precursor solution was prepared from Strontium (II) acetate and Titanium (IV) oxide acetylacetonate in propionic acid, acetylacetone, and 2-methoxyethanol. Strontium (II) acetate was dissolved in propionic acid and acetylacetone, then combined with a solution containing Titanium (IV) oxide acetylacetonate with 2-methoxyethanol. This mixture was heated to 60 °C for 10 min with continuous stirring to obtain a stable yellow-colored solution with a total cation concentration of 0.3 M. Further dilution with the above-obtained mixture solvents prepared 0.006 M STO precursor solution to be used to seeded nucleation. This precursor solution was poured into a porcelain boat, followed by annealing at 970 °C for 4 h in three different atmospheres, including Ar–4%H_2, Ar, and air to fabricate the STO powders after heated at 120 °C for several hours to remove most of solvents in ambient atmosphere. To the larger lattice mismatch with Ni–W substrate, seeded nucleation was utilized to enable oriented growth of STO films [4]. Therefore, the STO precursor solution with a total cation concentration of 0.006 M was spin-coated onto short textured Ni–W substrate of 1 × 1 cm in size at 3000 rpm for 30 s. As-coated STO precursor sample was annealed at 1000 °C for 10 min in a reducing forming gas atmosphere of Ar–4%H_2 to prepare STO seed layer. Then the final STO film was deposited by spin coating the 0.3 M STO precursor solution onto the above-mentioned STO seed layer at 2500 rpm for 30 s, followed by heat treatment at 970 °C for 80 min in a flowing gas mixture of Ar–4%H_2. Then the sample was cooled down to room temperature in the same reducing forming gas atmosphere of Ar–4%H_2.

The thermal decomposition process of STO precursor gel (obtained by heating the precursor solution at 120 °C for several hours to remove the solvents) was measured by differential scanning calorimetry (DSC) and thermogravimetric analysis (TGA), in which a heating rate of 20 °C min^{-1} was used in flowing nitrogen at 100 mL min^{-1}. Fourier transform infrared (FT-IR) spectra were recorded at room temperature on a measurement system EQUINX55 in the wave number range of 4000–400 cm^{-1} with a resolution of 2 cm^{-1}. The transmission electron microscopic (TEM) analysis was carried out using a JEM-2100 FS operating at 200 keV to obtain the images. XRD θ–2θ scans from CuKα radiation at 40 kV and 50 mA identified phase purity, crystallinity of the STO powders, films, and epitaxial growth of films. In addition, the STO film and its underlying Ni–W substrate were also characterized by XRD, which was performed to carry out out-of-plan scan for the texture degree. The film thickness of STO was calibrated and determined by α-step apparatus. JSM-6700 field emission scanning electron microscopy (SEM) and a digital instruments nanoscope SPI3800-SPA-400 atomic force microscopy (AFM) in contact mode documented the STO film surface morphology.

Results and discussion

The thermal decomposition behavior of the STO precursor gel (afforded by heating the precursor solution at 120 °C for several hours to remove solvents) was measured to obtain useful information on the decomposition process of the deposited precursor film and to establish a suitable heat treatment schedule. As shown in Fig. 1, the weight loss in the TG curve and endothermic peak in the DSC curve below 180 °C were caused by volatilization of the rudimental solvents. The strong endothermic peaks at 270 and 360 °C in DSC curve correlated very well with the rapid weight loss signals of the DTG curve (derivative of the TG curve after the temperature), which may result from the decomposition of precursors. Whereas the endothermic peak at 750 °C and exothermic peak at 930 °C in DSC curve were not associated with any obvious mass loss, which corresponds most likely to the transition of crystallization morphology and the formation of STO oxide out of

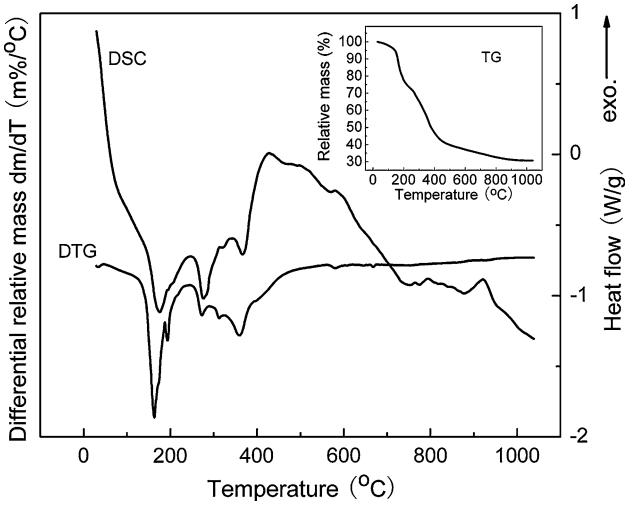

Fig. 1 DSC and DTG curves of STO precursor gel measured with a heating rate of 20 K min^{-1} in nitrogen

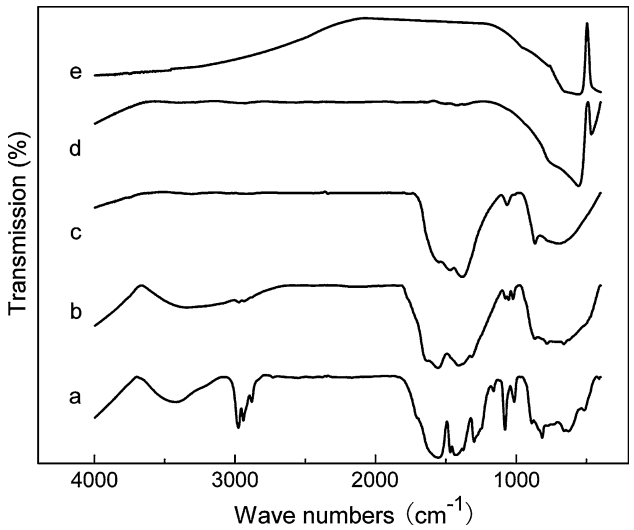

Fig. 2 FT-IR spectra of (*a*) the as-prepared STO precursor gel and its powders annealed at (*b*) 270 °C, (*c*) 360 °C, (*d*) 750 °C, and (*e*) 970 °C, respectively

SrO and TiO_2. The maximum decomposition temperature is 970 °C. It indicates that the complete crystallization temperature of STO precursor gel may be nearly 970 °C in this new precursor solution route. The decomposition of a stoichiometric mixture of the starting precursors with Sr:Ti = 1:1 would lead to a total mass loss of around 62.22%, which is lower than the observed 69.34%. The reaction between the educts and solvents in precursor solution may take place during the preparation process of STO precursor solution.

In order to understand the possibility of the reaction in STO precursor solution and the decomposition behavior of STO precursor gel, FT-IR spectroscopy measurements were performed on the decomposed powders at different temperatures, at about which obvious endothermic or exothermic peaks were observed from the DSC curve, as shown in Fig. 2. In Fig. 2a, the typical bands of the acetate could be observed at 1557 cm^{-1}, which is assigned to the asymmetric stretching vibration COO^-. Furthermore, the typical vibration bands for acetate were found at 1075, 895, and 819 cm^{-1}. The presence of pentanedionates could be excluded due to the absence of the coupled stretching vibrations of C–C and C–O at around 1592 and 1525 cm^{-1} [18]. And the IR absorption bands at 1166 and 1016 cm^{-1} are corresponding to O–C–O stretching vibration, which can be attributed to the existence of 2-methoxyethanoxide. The absorption band at 3420 cm^{-1} is assigned to C–O stretching vibration, while all of the absorption bands at 2980, 2940, 2879, and 1466 cm^{-1} are attributable to C–H stretching vibration. The IR absorption band at 1303 cm^{-1} is corresponding to O–H bending vibration, which may result from the rudimental solvent. Pure metal–oxygen stretching vibrations can be found at wave numbers of 639 and 512 cm^{-1} [19]. As a result, It could be concluded that the acetylacetonate were converted into 2-methoxyethanoxide during the preparation of precursor solution, which is in good agreement with the presumption from the TG measurements. Figure 2b shows the FT-IR reflectivity spectrum of the precursor powder annealed at 270 °C, which is identical to that of the as-synthesized precursor gel except the disappearance of the absorption band at 1303 cm^{-1} and the less intensity of all of vibration bands. It suggests that the rudimental 2-methoxyethanol in precursor gel evaporates at the annealing temperature of 270 °C and there is no obvious alteration of the powdered product. As can be clearly seen from Fig. 2c, the absorption bands at 3420, 2980, 2940, 2879, and 1166 cm^{-1} disappeared when the annealing temperature of STO precursor gel increased to 360 °C. As the annealing temperature increased further to 750 °C, the vibration bands at 1557, 1466, 1075, and 1016 cm^{-1}, which is attributed to organic constituents, disappeared completely. With increasing annealing temperature of the STO precursor gel to 970 °C, however, the vibration band at about 471 cm^{-1}, which is tentatively attributed to Sr–O, disappears along with a little shift of Ti–O vibration band at around 564 cm^{-1} towards the low wave numbers. This change can be explained by the weaker interaction between Ti and oxygen atom in STO structure than that in TiO_2 simple oxide, while the interaction between Sr and oxygen atom in STO structure may be too weak to be detected its obvious infrared spectral feature. It indicates that decomposition of the organic constituents in precursor powders almost finished up to 750 °C, which correlates with the results achieved by the TGA measurements. Moreover, the STO

phase may completely synthesize from the simple oxides of Sr and Ti and crystallized at a high temperature of 970 °C. These results are in good agreement with the TG–DSC analysis of its precursor gel.

High resolution TEM investigations of STO powders annealed at different temperatures were carried out and illustrated in Fig. 3 to analyze the transition from gel state to crystalline material. As shown in Fig. 3a, STO powder annealed at 270 °C is unstable and quickly damaged by the electron beam. There is no obvious difference in respect of the images between the STO powders annealed at 360 and 270 °C even though the former further tends to blow up and burst open completely. Some particles with an average size of 25 nm are found from the image of STO powder annealed at 750 °C. It can be considered that as-observed some small particles may be the oxides nuclei or carbon residues due to the presence of only metal–oxygen vibration bands in the FT-IR spectrum of STO powder annealed at 750 °C [20]. However, the STO powder annealed at 970 °C completely crystallizes because of the observed series of scattered diffraction spots in Fig. 3d [21, 22].

From the above-discussed TGA–DSC, FT-IR, and TEM analyses, it can be concluded that the decomposition of STO precursor gel almost completes and forms plenty of the simple oxides of Sr and Ti at the annealing temperature of 750 °C. Moreover, a possible nucleation of STO phase begins at below 750 °C. However, the STO phase could not completely crystallize until the annealing temperature increases to nearly 970 °C. In other words, the crystallization of STO phase, which may occur along with the combination of simple oxides of Sr and Ti in the range of 750 to 970 °C, undergoes a wide temperature interval. Therefore, we selected 970 °C as our crystallization temperature for a long annealing time to fabricate STO crystallized powders and STO oriented film at this temperature. It should be pointed out that the preparation of STO film was achieved by adopting a seeded nucleation method. And many tests also showed that if the STO film from precursor solution with a relative high concentration was deposited directly on to Ni–W substrate for a short annealing time, the texture of the resulted STO film was bad. It can be considered that in this case its large lattice mismatch (around 11%) with Ni–W substrate and the wide temperature range of crystallization process of STO precursor gel result in the random nuclei formation in the bulk of the film and the inhomogeneity of the STO amorphous phase, and then give rise to the bad texture of final crystallized film, while the seeded nucleation method and prolonging the annealing time could prevent from this bad effect [4].

The powder X-ray diffraction analysis indicated that the single-phase STO powders were obtained in three kinds of annealing atmospheres, including Ar–4%H_2, Ar, and air, as shown in Fig. 4. It indicates that there is no obvious influence of the oxygen partial pressure on the structural stability of STO. And it is possible that STO with the perovskite structure is prone to tolerate the oxygen vacancies defect. Figure 4 also shows the normalized intensity of the (110) diffraction peak for STO powders fabricated in Ar–4%H_2, Ar, and air, respectively. The full width at half-maximum (FWHM) values decrease, and this is accompanied by the shift of the STO (110) diffraction peak positions towards higher diffraction angles as the oxygen partial pressure in annealing atmosphere increases. It is highly possible that the crystallization degree of STO powders increase along with the decrease of carbon

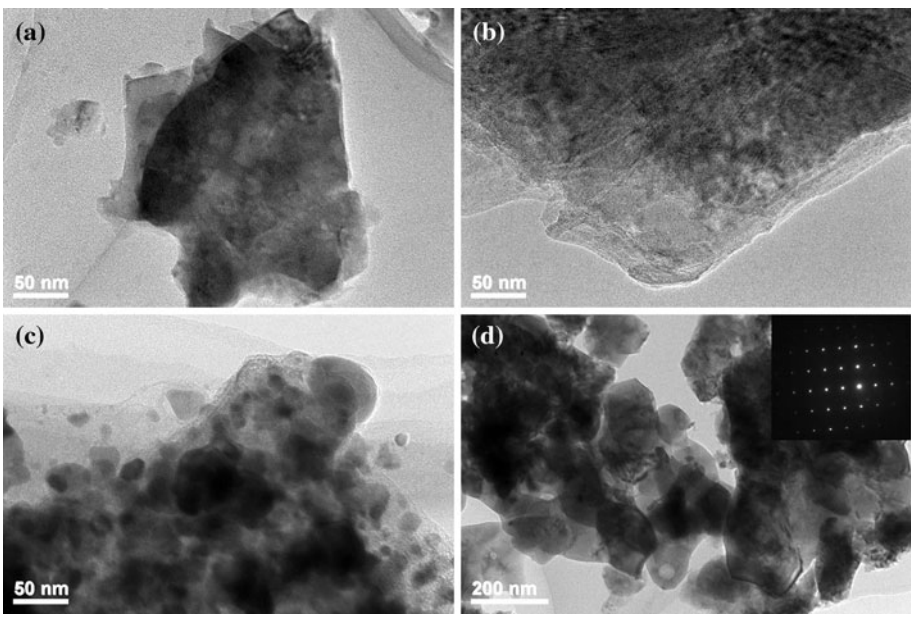

Fig. 3 TEM analyses of the STO powders annealed at **a** 270 °C, **b** 360 °C, **c** 750 °C, and **d** 970 °C, respectively

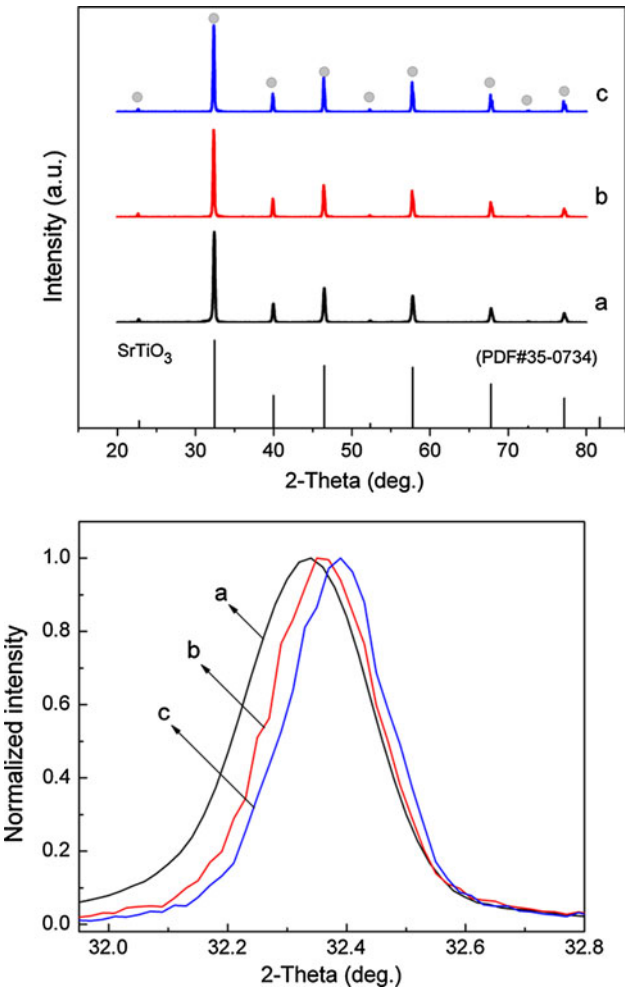

Fig. 4 X-ray diffraction patterns and the normalized intensity of the (110) diffraction peak for STO powders fabricated in **a** Ar–4%H_2, **b** Ar, and **c** air, respectively

residues as the oxygen partial pressure in calcination atmosphere increases [17].

Figure 5 shows X-ray diffraction patterns for STO seed layer and final STO crystallized film grown on textured Ni–W substrate. The STO seed layer prepared from 0.006 M precursor solution may be too thin to be detected its diffraction peaks by the present XRD technique due to the limited resolution. However, the only (00*l*) diffraction peaks of STO film and Ni–W substrate are visible in Fig. 5b, which illustrates that STO coating completely crystallize to form the preferred *c*-axis oriented film by seeded nucleation method using a newly developed precursor solution route. For the final STO crystallized film on Ni–W substrate fabricated by seeded nucleation method, its thickness calibrated by α-step apparatus is nearly 78 nm. An indication of the out-of-plane orientation can be found in the rocking curve of the (002) STO and the (002) Ni–W reflections, as shown in Fig. 6. The FWHM value of this (002) STO reflection is 5.21°, which means the

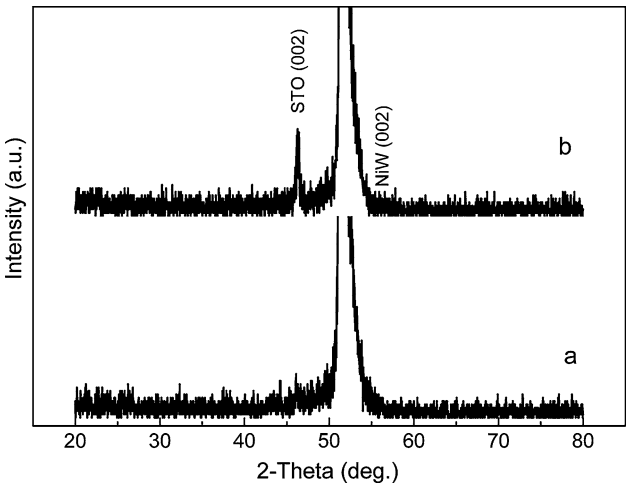

Fig. 5 The θ–2θ scans of STO seed layer and the final STO crystallized film on textured Ni–W substrate

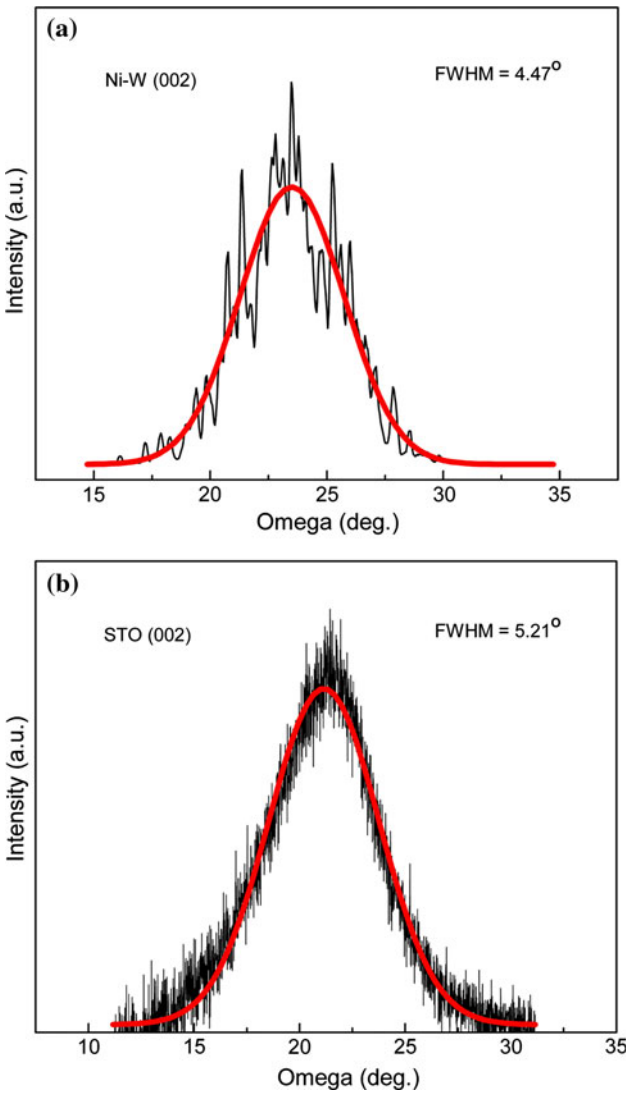

Fig. 6 The out-of-plane scans of the Ni–W (002) (**a**) and STO (002) (**b**) reflection of a STO buffer layer on Ni–W substrate annealed at 970 °C

out-of-plane misalignment is low, while the FWHM for underlying Ni–W (002) is 4.47°. The FWHM value of STO film is slightly greater in comparison to that of the Ni–W substrate. It indicates that STO film prepared by a new precursor solution method shows a good texture transfer from the substrate. This may be related to the special deposition route of STO film and the large mismatch between STO and Ni–W substrate, although allowing a good epitaxial growth on textured Ni–W substrate. Surface morphology of STO seed layer and its final crystallized film were investigated by SEM and AFM, as shown in Fig. 7. It can be found that the surface of Ni–W substrate is not fully covered by the STO seed layer, for which, the isolated islands have an average grain size of 130 nm and the average distance among these islands is about 150 nm as shown in Fig. 7a. However, the final STO crystallized film provides a good coverage for the Ni–W substrate surface, and most of the Ni–W grain boundary grooves on the Ni–W surface are found to be well covered. Moreover, Fig. 7b also shows that the final STO crystallized film is continuous, homogenous as well as crack-free. AFM image of the STO crystallized film grown on STO seed layer is shown in Fig. 7c. It reveals a root-mean-square roughness (Ra) of the final STO crystallized film as 4.31 nm, which can meet the requirement for subsequently deposited superconducting layers.

The results discussed for STO indicate that STO with perovskite structure is very stable due to its good tolerance for the oxygen vacancies defect. In addition, the high-quality STO film grown using the newly developed precursor solution route has a great deal of advantage as a buffer layer for YBCO-coated conductors, especially for a single buffer layer because of its very small lattice mismatch with YBCO layer and its low oxygen diffusivity [4].

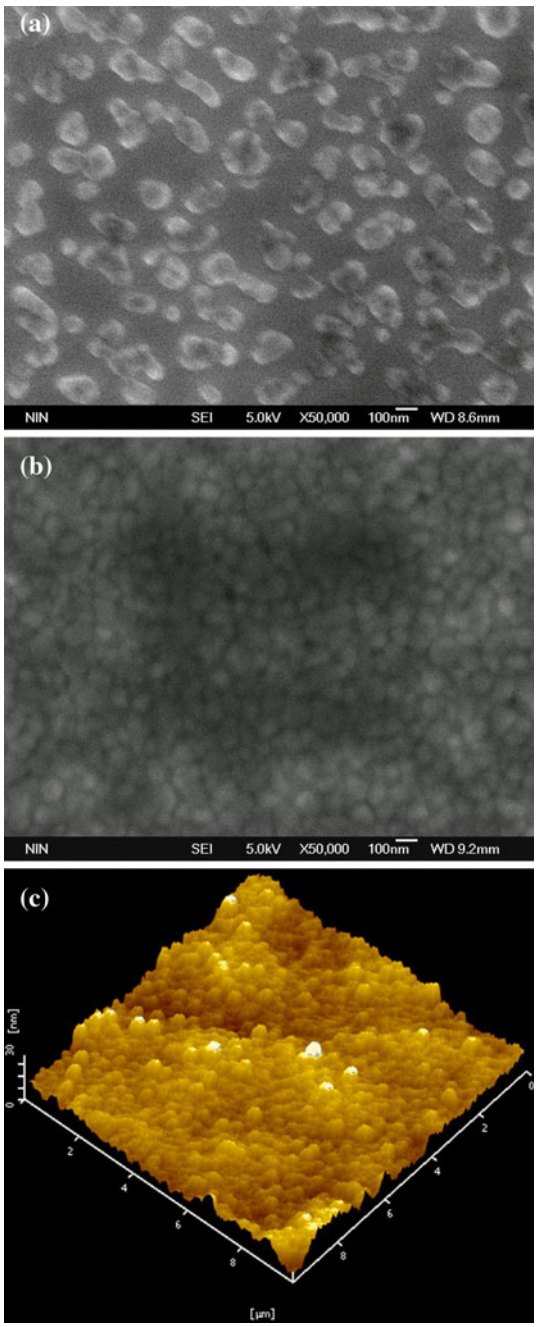

Fig. 7 **a** SEM image for STO seed layer, **b** SEM micrograph, and **c** AFM image of the final STO crystallized film grown on STO seed layer

Conclusions

We have successfully developed a new precursor to prepare STO by chemical solution approach. The investigation of TG–DSC analysis of the STO precursor gel, the FT-IR spectroscopy, and TEM measurement of its precursor gel as well as powders annealed at different temperatures provided a good understanding for the exact nature of the precursor solution chemistry, the decomposition, and crystallization behavior of STO precursor gel. A conversion of the acetylacetonate to 2-methoxyethanoxide took place during the synthesis process of STO precursor solution. The synthesis of STO single-phase powders at different atmospheres indicates that the structural stability of STO is very great. Furthermore, a good epitaxial STO film with continuous and crack-free morphology on textured Ni-W substrate has been obtained. It suggests that chemical solution deposited STO film using a new precursor could be used as buffer layer towards developing all-MOD architectures of buffer and superconducting layers in coated conductors.

Acknowledgements This study was financially supported by the National Science Fund Program and National 863 Program of China (Grant Nos. 50872115 and 2008AA03Z202).

References

1. Aytug T, Wu JZ, Kang BW, Verebelyi DT, Cantoni C, Specht ED, Goyal A, Paranthaman M, Christen DK (2000) Physica C 340:33
2. Uchida T, Watanabe S, Uchiyama T, Tachiki T (2008) J Phys Conf Ser 97:012057
3. Zhou YX, Bhuiyan S, Scruggs S, Fang H, Mironova M, Salama K (2003) Supercond Sci Technol 16:901
4. Dawley JT, Ong RJ, Clem PG (2002) J Mater Res 17(7):1678
5. Pomar A, Coll M, Cavallaro A, Gàzquez J, González JC, Mestres N, Sandiumenge F, Puig T, Obradors X (2006) J Mater Res 21(5):1106
6. Siegal MP, Clem PG, Dawley JT, Richardson J, Overmyer DL, Holesinger TG (2005) J Mater Res 20(4):910
7. Dawley JT, Clem PG (2002) Appl Phys Lett 81(16):3028
8. Sathyamurthy S, Salama K (2000) Supercond Sci Technol 13:L1
9. Zhu XB, Chen L, Liu SM, Song WH, Sun YP, Shi K, Sun ZY, Chen S, Han Z (2004) Physica C 415:57
10. Chen S, Sun Z, Shi K, Wang S, Meng J, Liu Q, Han Z (2004) Physica C 412–414:871
11. Zhu XB, Liu SM, Hao HR, Chen L, Song WH, Sun YP, Shi K, Sun ZY, Chen S, Han Z (2004) Physica C 411:143
12. Sathyamurthy S, Salama K (2002) Physica C 377:208
13. Pontes FM, Leite ER, Lee EJH, Longo E, Varela JA (2001) J Eur Ceram Soc 21:419
14. Celik E, Yamada Y, Hirabayashi I, Shiohara Y (2004) Mater Sci Eng B 110:94
15. Zheng ZK, Huang BB, Qin XY, Zhang XY, Dai Y (2011) J Colloid Interface Sci 358:68
16. Da Silva LF, Bernardi MIB, Maia LJQ, Frigo GJM, Mastelaro VR (2009) J Therm Anal Calorim 97:173
17. Da Silva LF, Maia LJQ, Bernardi MIB, Andrés JA, Mastelaro VR (2011) Mater Chem Phys 125:168
18. Knoth K, Hühne R, Oswald S, Schultz L, Holzapfel B (2007) Acta Mater 55:517
19. Wurm R, Dernovsek O, Greil P (1999) J Mater Sci 34:4031. doi:10.1023/A:1004668016453
20. Cloet V, Feys J, Hühne R, Hoste S, Driessche IV (2009) J Solid State Chem 182:37
21. Wang XW, Zhang ZY, Zhou SX (2001) Mater Sci Eng B 86:29
22. Pang GKH, Tai CW, Wang Y, Liu WL, Song ZT, Feng SL, Chan HLW, Choy CL (2006) Curr Appl Phys 6:583